



PII S0008-8846(96)00202-5

ANALYSES AND MODELS OF THE AUTOGENOUS SHRINKAGE OF HARDENING CEMENT PASTE II. MODELLING AT SCALE OF HYDRATING GRAINS

C. Hua¹, A. Ehrlacher¹ and P. Acker²

¹CERAM-ENPC, Central IV, 1 Av. Montaigne, 93167 Noisy-le-Grand Cedex, France

²LCPC, 58 Bd. Lefebvre, 75732 Paris Cedex, France

(Refereed)

(Received November 29, 1995; in final form December 17, 1996)

ABSTRACT

Our previous paper (Hua/1995/) has studied the autogenous shrinkage at macroscopic scale. One can also model the autogenous shrinkage at the scale of the hydrating grains without going into the colloidal details of the hydrates. At this scale, hydrates (including the immobilised water held by micropores) are considered as homogeneous isotropic viscoelastic and locally non-ageing. For the ensemble of the material, only the percentages of heterogeneities (hydrates, residual anhydrous cement, capillary water, etc.) vary during the process of hydration. The modelling is based on the mechanism of capillary depression for the same cement paste as that studied in the previous paper with a modelling at macroscopic scale (CPA 55 with W/C = 0.42). The result agrees well with measurement. © 1997 Elsevier Science Ltd

1. Introduction

The phenomenon of the autogenous shrinkage is similar to that of the drying shrinkage. There are three mechanisms to explain drying shrinkage (Powers/1965/, Wittmann/1976/, Baron/1982/):

1. Variation of capillary depression,
2. Variation of surface tension of colloidal particles,
3. Variation of disjoining pressure.

The last two mechanisms concern forces at colloidal particle scale and can explain drying shrinkage only qualitatively. The first mechanism often gives estimates of drying shrinkage that are much smaller than the measured values.

Our previous study (Hua/1995/), modelling of the autogenous shrinkage at macroscopic scale, has quantitatively demonstrated the capillary effect that causes a tension (depression) in the liquid phase and so induces a shrinkage (compression) of the solid skeleton according to the first mechanism. In that study, the ensemble of the hardening cement paste (anhydrous residual cement, hydrates and water) is considered as an ageing viscoelastic homogeneous

material. This paper also takes into account the mechanism of capillary depression (Hua/1995/, Crassous *et al.* /1993/ and Tazawa *et al.*/1993/) and would attempt to confirm, at another viewpoint (micro-mechanics), that the capillary effect is the main cause of the auto-genous shrinkage).

Once more, we try to model a macroscopically ageing material by its constituents supposed to be microscopically non-ageing. It is well known that hydrates have some intrinsic properties (internal porosity, specific surface area etc.) and are always saturated in water during hydration (Hua/1992/, /1995/, Baroghel-Bouny/1994/, Powers/1960/ and Jennings/1983/). The hydrates (including the immobilised water held by micropores) can therefore be regarded as homogeneous isotropic viscoelastic and locally non-ageing without going into the details of their microstructure. Thus one supposes that cement paste is made up of continuous, homogeneous, isotropic and non-ageing constituents, and that only the percentages of the constituents vary during the hydration. The heterogeneous medium is presented by Figure 1 with:

1. "Anhydrous cement" considered as elastic
2. "Hydrates and immobilised water" considered as viscoelastic
3. "Capillary water" exerting a capillary depression on the solid skeleton
4. "Gaseous spaces" supposed to be in the form of bubbles; they do not appear in this model because the bubbles of water vapour have no direct effect on the solid skeleton, and can be replaced by the water under the same capillary depression (see Hua/1992/)

So we have to deal with a problem of material exchange (evolutional boundaries between different phases: hydrates, residual anhydrous cement and water). There are two principal difficulties when a finite element method (FEM) is used:

1. In a representative volume element, there are too many hydrating cement grains.
2. It is difficult to impose the boundary conditions, particularly the boundary liquid/solid.

A periodical distribution of spherical anhydrous cement grains is adopted in order to overcome the first difficulty (detailed in section 3). Indeed, the model of spheres embedded in a matrix is largely employed to study effective properties of an heterogeneous material, such as *Young's* module E_{eff} , *Poisson's* ratios ν_{eff} etc., but there is no material exchange (fixed

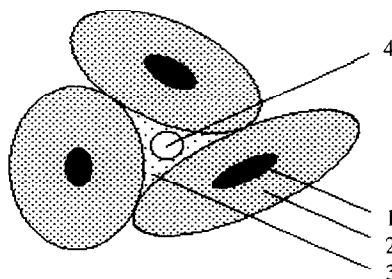


FIG. 1.
Schema of cement paste at scale of grains.

interfaces) between inclusions and matrix for this type of problems (see Christensen/1979/, Roelfstra/1988/). This paper describes an hydro-mechanical coupled problem with material exchange and it is useful to point some interesting advantages of our iterative process (detailed in section 5) from algorithmic viewpoint:

1. The division of finite elements remains unchanged for the whole calculation.
2. The boundaries on which we impose the boundary conditions remain unchanged.
3. The global stiffness matrix remains unchanged.

2. Development of a Hydrating Grain

The hydration is a procedure of the solid volume development. It is therefore necessary, for the model, to know the volumes of components during hydration. To simplify the presentation, the following notation is used:

$V_c(t)$: volume of residual anhydrous cement

$V_{ch}(t)$: volume of hydrated cement $V_{ch}(t) = V_c(0) - V_c(t)$

$V_w(t)$: current water volume

$V_{wh}(t)$: volume of chemically bonded water $V_{wh}(t) = V_w(0) - V_w(t)$

$V_h^{ap}(t)$: apparent volume of hydrates

ρ_r : ratio of the density of cement to that of water ρ_c/ρ_w (≈ 3.1)

W : mass of water

C : mass of cement

It is easy to obtain the next equation by taking into account the quantity of chemically bonded water, the *Le Chatelier* contraction, and the intrinsic porosity (28%) of the hydrates (Hua/1992/).

$$V_h^{ap}(t) = 2.156 V_{ch}(t) \quad (1)$$

In cement chemistry, one distinguishes inner hydrates and outer hydrates. Equation (1) means that one volume of anhydrous cement produces two volumes of hydrates, one of which forms *in situ*, by destroying the anhydrous cement, while the other passes through the porous layers of hydrates and precipitates outside the grain. The solid volume thus develops progressively. This is shown by Figure 2 with:

1. Hydrates at time t
2. Anhydrous cement at time t
3. New external hydrate at time $t + \Delta t$
4. New internal hydrate at time $t + \Delta t$

3. Distribution of Grains and Time of Setting

In our model, the initial state is the time of setting when a skeleton forms and begins to undergo the capillary depression due to self-desiccation (Hua/1992/ and Hua et al./1995/). To simplify the model, it is supposed that all grains of anhydrous cement are spherical and

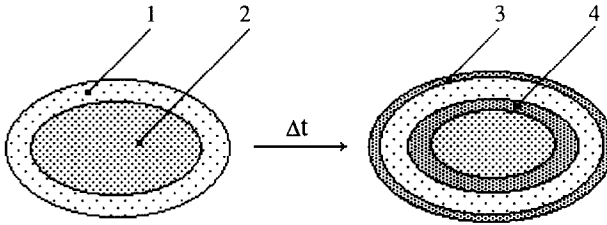


FIG. 2.

Diagram of the development of a cement grain.

identical, and that the distribution of grains is periodic. The assumption of periodicity allows us to work on a periodic cell. When hydrating grains (a core of anhydrous cement with layers of hydrates) touch each other, it is the time of setting.

At first, the degree of hydration at the time of setting is studied for two particular distributions. The degree of hydration is defined by:

$$\alpha(t) = \frac{V_c(0) - V_c(t)}{V_c(0)} = \frac{V_{ch}(t)}{V_c(0)} \quad (2)$$

With a simple cubical distribution and the condition $r_{in} \leq l/2$ (r_{in} being the initial radius of an anhydrous cement grain and l being the length of cube), by taking equation (1) into account, we can obtain the degree of hydration for $W/C = 0.42$ at the time of setting t_0 :

$$\alpha(t_0) = \frac{(1 + \rho_r W/C)\pi/6 - 1}{1.156} = 17.76\% \quad (3)$$

With a centred cubical distribution and the condition $r_{in} \leq \sqrt{3}l/4$, the same calculation gives:

$$\alpha(t_0) = \frac{(1 + \rho_r W/C)\sqrt{3}\pi/8 - 1}{1.156} = 48.94\% \quad (4)$$

In general cases, observations indicate that setting takes place when the degree of hydration reaches approximately 20%, whatever the W/C ratio (Jennings/1983/). The simple cubical distribution is therefore regarded as closer to reality for cement paste with $W/C = 0.42$, and this distribution will be used for the numerical modelling. Because of the symmetry of the cell, we can take an eighth of a sphere in a unit cube as shown by Figure 3.

4. Mechanical Model of the Cement Paste

In the mechanical model, the material is composed of three constituents with locally non-ageing properties:

Anhydrous cement. This component is considered as elastic isotropic; its behaviour is therefore characterised by a stiffness tensor $A_{ijkl}(E_a, \nu_a)$ depending on E_a (Young's modulus of

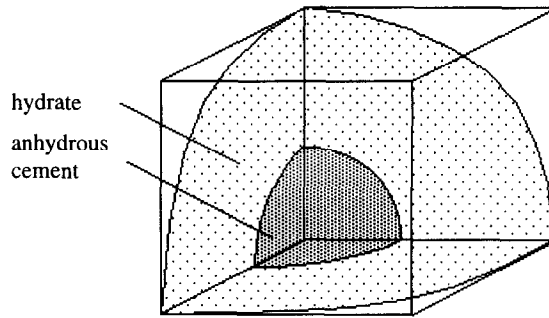


FIG. 3.

Diagram of an eighth of hydrating grain at the time of setting.

anhydrous cement) and ν_a (*Poisson's ratio of anhydrous cement*). It is successively replaced by internal hydrate layers.

Hydrates and immobilised water. The ensemble is considered as a viscoelastic isotropic component, corresponding to the *Zener* model shown by Figure 4. Its behaviour is therefore represented by three stiffness tensors $H_{ijkl}^1(E_{h1}, \nu_{h1})$, $H_{ijkl}^2(E_{h2}, \nu_{h2})$, and $\eta_{ijkl}(\eta, \nu_\eta)$. Each of these tensors depends on two characteristic parameters of the isotropic material. The viscoelastic deformation of each layer of hydrates begins when it forms. Each new layer is deposited on layers already deformed by the capillary depression. Therefore each hydrate layer itself has a history of deformation. This effect can be taken into consideration by different initial deformations introduced in each layer.

Capillary water. This water exerts a capillary depression on the solid skeleton, and it is replaced gradually by external hydrate layers (the part of voids can be replaced by water under the same capillary depression for the reason stated previously).

Since the precipitation of dissolved hydrates occurs in the liquid phase under spherical stress, the following hypothesis is framed:

Hypothesis. For each hydrate layer, the deviatoric stress is zero ($\text{dev}(\sigma_{ij}) = 0$) when the layer forms. Then each layer begins to deform according to the viscoelastic law of the *Zener* model.

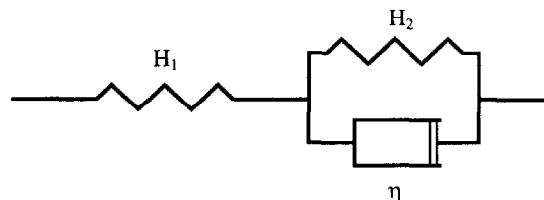


FIG. 4.

Rheologic model of viscoelastic material.

5. Numerical Simulation by the Finite Element Method

5.1 Idea of the Model. We divide a period of hydration into steps $t_0, t_1, t_2, \dots, t_N$. At each step, a homogeneous elastic calculation is done with the instantaneous stiffness of hydrates $H_{ijkl}^1(E_{h1}, \nu_{h1})$ for the whole cube, the deformation $\epsilon_{ij}^e(t)$ is then obtained. Since the material is not homogeneous, each phase has a different behaviour, and each hydrate layer itself has a history. So we introduce two supplementary terms, $\epsilon_{ij}^i(t)$ and $\epsilon_{ij}^v(t)$, to take these effects into account. In this way, the real deformation and the real stress are obtained.

$$\epsilon_{ij}(t) = \epsilon_{ij}^e(t) + \epsilon_{ij}^i(t) + \epsilon_{ij}^v(t) \quad (5)$$

$$\sigma_{ij}(t) = H_{ijkl}^1 \left[\epsilon_{kl}(t) - \epsilon_{kl}^i(t) - \epsilon_{kl}^v(t) \right] \quad (6)$$

At each iteration, these supplementary terms $\epsilon_{ij}^i(t)$ and $\epsilon_{ij}^v(t)$ are updated as follows:

- *In the water phase.* The deformation $\epsilon_{ij}^v(t)$ is zero, the deformation $\epsilon_{ij}^i(t)$ is updated to cancel the deviatoric stress since the stress is spherical in the liquid phase.
- *In the anhydrous cement phase.* The deformation $\epsilon_{ij}^v(t)$ is equally zero, but the deformation $\epsilon_{ij}^i(t)$ is updated to rigidify the material because the true stiffness of this phase is the tensor $A_{ijkl}(E_a, \nu_a)$ instead of the tensor $H_{ijkl}^1(E_{h1}, \nu_{h1})$ with which the homogeneous elastic calculation is effected for the whole cube.
- *In the hydrates phase.* The deformation $\epsilon_{ij}^v(t)$ evolves according to the viscoelastic law of the Zener model, while the deformation $\epsilon_{ij}^i(t)$ no longer varies and is fixed, in each hydrate layer, to cancel the deviatoric stress at the instant of the creation of this hydrate layer (according to the hypothesis in the section 4). Therefore the term $\epsilon_{ij}^i(t)$ is introduced to take into account the precipitation of hydrate layers under spherical stress at different instants.

Remark:

The fact of taking the same stiffness $H_{ijkl}^1(E_{h1}, \nu_{h1})$ in the water phase as in the hydrates phase has no importance because it is sufficient, in this zone, to have a spherical stress field. The equilibrium boundary conditions will impose a spherical stress $-p_c \delta_{ij}$.

5.2 Discrete Process.

a. Discretization of time $[t_0, t_N]$. For the cement paste with W/C = 0.42, the autogenous shrinkage (or precisely, shrinkage of hydration) is measured during a period of 25 days. This period is therefore taken as $[t_0, t_N]$, where t_0 is the time of setting and t_N is equal to 25 days.

Using a regression function based on measures of the degree of hydration $\alpha(t)$ (Hua/1992/ and Hua et al. /1995/), and assuming that all anhydrous cement grains are

Table 1. Discretization of time, layers and loads

t_n (day)	$\alpha(t_n)$ (%)	$a(t_n)$	$h(t_n)$	$p_c(t_n)$ (MPa)	$\overline{p_c(t_n)}$ (MPa)
0.1556	17.76	0.8804	1.000	0.0000	/
0.1970	22.12	0.8645	1.014	0.1327	0.0664
0.2500	26.32	0.8487	1.028	0.2667	0.1997
0.3182	30.36	0.8329	1.041	0.4023	0.3345
0.4063	34.26	0.8171	1.054	0.5399	0.4711
0.5212	38.00	0.8012	1.067	0.6798	0.6098
0.6720	41.60	0.7854	1.080	0.8227	0.7513
0.8722	45.06	0.7696	1.092	0.9694	0.8961
1.1420	48.38	0.7538	1.104	1.2385	1.1039
1.5110	51.57	0.7379	1.116	1.7854	1.5119
2.0290	54.62	0.7221	1.127	2.5318	2.1586
2.7790	57.54	0.7063	1.139	3.4730	3.0024
3.9180	60.33	0.6905	1.149	4.6087	4.0409
5.7890	62.99	0.6746	1.160	5.9475	5.2781
9.3570	65.54	0.6588	1.171	7.5174	6.7324
20.670	67.94	0.6430	1.181	9.4354	8.4764

spherical and identical, we can calculate the radius of residual anhydrous cement grains $a(t_n) \in [a(t_0), a(t_N)]$ at a given instant $t_n \in [t_0, t_N]$.

The period $[t_0, t_N]$ is divided into 15 steps in this way that we can have 15 identical thickness layers between two radii $[a(t_0), a(t_N)]$ to facilitate the division.

The discretization of time t_n is presented in Table 1. The degree of hydration $\alpha(t_0)$ and the radius of residual anhydrous cement grains $a(t_0)$ are calculated for the simple cubical distribution. The degree of hydration $\alpha(t_N)$ ($t_N = 25$ days) is measured and the corresponding radius $a(t_N)$ is calculated for the same distribution. The instant t_N in Table 1 does not correspond precisely to 25 days because the instants t_n are calculated from a regression function $\alpha(t)$ that does not pass through all the measured points.

b. Centric Division of Zones. Let us consider a unit cube in which is positioned an eighth of a sphere (hydrating cement grain), and note that $a(t_n)$ is the radius of residual anhydrous cement grains and $h(t_n)$ is the radius of the interface between external hydrates and capillary water at step n . The cube can be divided into five zones, as shown by Figure 5.

Zone 1 ($0 \leq r \leq a(t_N)$): residual anhydrous cement

Zone 2 ($a(t_N) < r \leq a(t_0)$): internal hydrates and anhydrous cement

Zone 3 ($a(t_0) < r \leq h(t_0)$): hydrates formed before setting

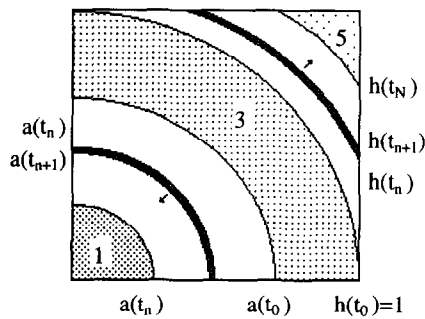


FIG. 5.
Different zones in the cube.

Zone 4 ($h(t_0) < r \leq h(t_N)$): external hydrates and capillary water

Zone 5 ($h(t_N) < r$): capillary water

Zones 2 and 4 are transitory, because during the period $[t_0, t_N]$, the anhydrous cement (in zone 2) is successively replaced by internal hydrate layers and the water (in zone 4) is gradually replaced by external hydrate layers. At time t_N , both zones 2 and 4 are totally occupied by hydrates. Zones 1, 3 and 5 are homogeneous.

With the relation $V_n^{op}(t) = 2.156 V_{ch}(t)$ (equation 1), one can easily calculate the $h(t_n)$ corresponding to $a(t_n)$. This is also shown by Table 1.

c. Discretization of Loads. The load in the boundary conditions is calculated from the capillary depression obtained from experimental measures (Hua/1992/ and Hua et al./1995/). For each instant t_n , using a regression function of the capillary depression $p_c(t_n)$, the corresponding load (Table 1) can be calculated. We keep a constant load at each step $[t_n, t_{n+1}]$. This load is given by the last column of Table 1, calculated by the following equation:

$$\overline{p_c(t_n)} = \frac{1}{2} [p_c(t_n) + p_c(t_{n+1})]$$

d. Material Parameters. The following material parameters are used.

Elastic stiffness for the anhydrous cement $A_{ijkl}(E_a, \nu_a)$

Instantaneous stiffness of hydrates $H_{ijkl}^1(E_{h1}, \nu_{h1})$

Viscoelasticity of hydrates $H_{ijkl}^2(E_{h2}, \nu_{h2}), \eta_{ijkl}(\eta, \nu_\eta)$

where E_a, E_{h1}, E_{h2} are Young's moduli, $\nu_a, \nu_{h1}, \nu_{h2}, \nu_\eta$ are Poisson's ratios and η is the viscosity of hydrates.

By making the following two hypotheses, one can decrease the number of parameters and so simplify the mathematical formulation (Hua /1992/).

Hypothesis. For viscoelastic hydrates, the characteristic delay-times under pressure and under shear are equal.

$$\theta = \theta_\lambda = \theta_\mu$$

Hypothesis. The Poisson's ratios for the tensors $H_{ijkl}^1(E_{h1}, \nu_{h1})$, $H_{ijkl}^2(E_{h2}, \nu_{h2})$, $A_{ijkl}(E_a, \nu_a)$ are equal.

$$\nu = \nu_a = \nu_{h1} = \nu_{h2}$$

With these hypotheses, only five parameters (E_a, E_{h1}, E_{h2}, ν and θ) are needed for the calculation.

e. Problem to be Resolved from Step n to Step $n + 1$.

Boundary conditions. According to the hypothesis of periodicity and the symmetry, we impose the following conditions, shown in Figure 6.

On the faces $x = 1$, $y = 1$ and $z = 1$:

$$\text{if } \sqrt{x^2 + y^2 + z^2} < h(t_N): \begin{cases} u_i n_i = R(t_n) \\ \sigma_{ij} n_i t_j = 0 \end{cases} \quad (7)$$

$$\text{if } \sqrt{x^2 + y^2 + z^2} \geq h(t_N): \begin{cases} \sigma_{ij} n_i = -p_c(t_n) n_i \\ p_c(t_n) < 0 \end{cases} \quad (8)$$

with a self-equilibrium condition on these faces.

$$\int \sigma_m ds = 0 \quad (9)$$

On the faces $x = 0$, $y = 0$ and $z = 0$:

$$\begin{cases} u_i n_i = 0 \\ \sigma_{ij} n_i t_j = 0 \end{cases} \quad (10)$$

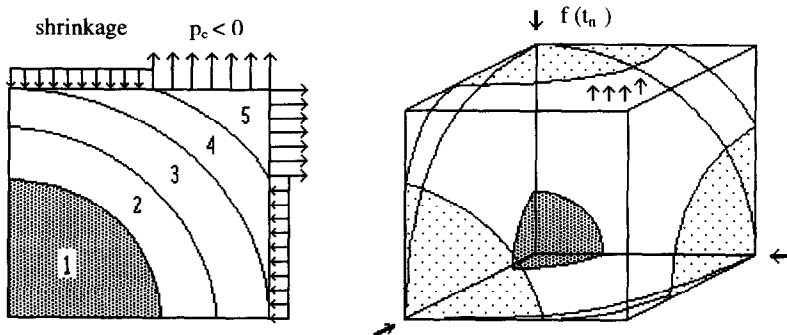


FIG. 6.

Boundary conditions imposed on the faces.

where

$R(t_n)$: uniform displacement to be determined (shrinkage)

n_i : normal vector of the face

t_i : tangent vector of the face

$p_c(t_n)$: known capillary depression at time t_n

Remark

The condition expressed by Equation (9) is realised by means of a concentrated force $f(t_n)$ and a perfectly rigid plate (as shown by Figure 6) with:

$$f(t_n) = p_c(t_n) \left(1 - \frac{\pi}{4} (h^2(t_n) - 1) \right) \quad (11)$$

Initial conditions. Initially ($n = 0$) the deformation $\epsilon_{ij}(t_0)$, $\epsilon_{ij}^i(t_0)$, and $\epsilon_{ij}^v(t_0)$ are zero. For any n , at the end of iteration, these deformations are obtained and used for the next step $n + 1$.

Development towards the step $n + 1$. By updating the terms $\epsilon_{ij}^i(t_{n+1})$ and $\epsilon_{ij}^v(t_{n+1})$, we can replace a layer of water between the radius $h(t_n)$ and the radius $h(t_{n+1})$ by an external hydrate layer and replace a layer of anhydrous cement between the radius $\alpha(t_n)$ and the radius $\alpha(t_{n+1})$ by an internal hydrate layer as shown by Figure 5. The iteration process is therefore as follows:

1⁰ Solve a homogeneous elastic and isotropic problem.

$$\sigma_{ij}(t_{n+1}) = H_{ijkl}^1 \left[\epsilon_{kl}(t_{n+1})^1 - \epsilon_{kl}^i(t_n) - \epsilon_{kl}^v(t_n) \right] \quad (12)$$

where $\sigma_{ij}(t_{n+1})^1$ and $\epsilon_{kl}(t_{n+1})^1$ are solutions of the problem and the superscript "1" means the first iteration.

2⁰ Update the terms $\epsilon_{ij}^i(t_n)$ and $\epsilon_{ij}^v(t_n)$ according to the idea presented above (section 5.1).

$$\epsilon_{ij}^i(t_n) \rightarrow \epsilon_{ij}^i(t_{n+1})^1 \quad \text{and} \quad \epsilon_{ij}^v(t_n) \rightarrow \epsilon_{ij}^v(t_{n+1})^1$$

3⁰ Recalculate a homogeneous elastic and isotropic problem.

$$\sigma_{ij}(t_{n+1})^{p+1} = H_{ijkl}^1 \left[\epsilon_{kl}(t_{n+1})^{p+1} - \epsilon_{kl}^i(t_{n+1})^p - \epsilon_{kl}^v(t_{n+1})^p \right] \quad (13)$$

with $p = 1, 2, \dots$

4⁰ Re-update the terms $\epsilon_{ij}^i(t_{n+1})^p$ and $\epsilon_{ij}^v(t_{n+1})^p$.

When the deformations $\epsilon'_{ij}(t_{n+1})^p$ and $\epsilon''_{ij}(t_{n+1})^p$ converge, we go to the next step.

This iteration process has some interesting advantages from an algorithmic viewpoint:

- The division of finite elements remains unchanged for the whole calculation.
- The boundaries on which the boundary conditions are imposed remain unchanged.
- The global stiffness matrix which corresponds to the tensor H^l_{ijkl} remains unchanged.

6. Evaluation of Material Parameters and Results

The material parameters of our numerical model are:

E_a : elastic modulus of anhydrous cement

E_{h1} : instantaneous elastic modulus of hydrates

E_{h2} : viscoelastic modulus of hydrates

θ : characteristic delay-time of hydrates ($\theta = \eta / E_{h2}$)

ν : Poisson's ratio

At the age of four weeks for the cement paste with W/C = 0.42 (regarded as hardened), the instantaneous elastic modulus E_{macro} is measured (Hua/1992/ and Hua et al./1995/):

$$E_{macro} = 17.63 \text{ GPa}$$

Note that the hydrate part is treated as a continuous medium (including the microporosity); if the capillary porosity is removed, we have:

$$E_{c+h} = 22.73 \text{ GPa}$$

As for individual moduli E_a and E_{h1} , we can use a formula for a granule-matrix mixture (see De Larrard/1991/).

$$E_{eff} = \frac{(1+g)E_g + (1-g)E_m}{(1-g)E_g + (1+g)E_m} E_m \quad (14)$$

TABLE 2
Groups of Material Parameters

Group	E_a (GPa)	E_{h1} (GPa)	E_{h2} (GPa)	θ (days)	ν
No. 1	40	20	20	30	0.2
No. 2	40	25	20	30	0.2
No. 3	40	23	20	35	0.2

where

E_{eff} : effective modulus of the mixture

E_g : elastic modulus of granule

E_m : elastic modulus of matrix

g : concentration of granule

Taking the hydrates as matrix and the residual anhydrous cement as granule, with $g = 0.1794$, assuming $E_a = 2E_m$ we have:

$$E_a = 40 \text{ GPa} \quad E_{h1} = 20 \text{ GPa}$$

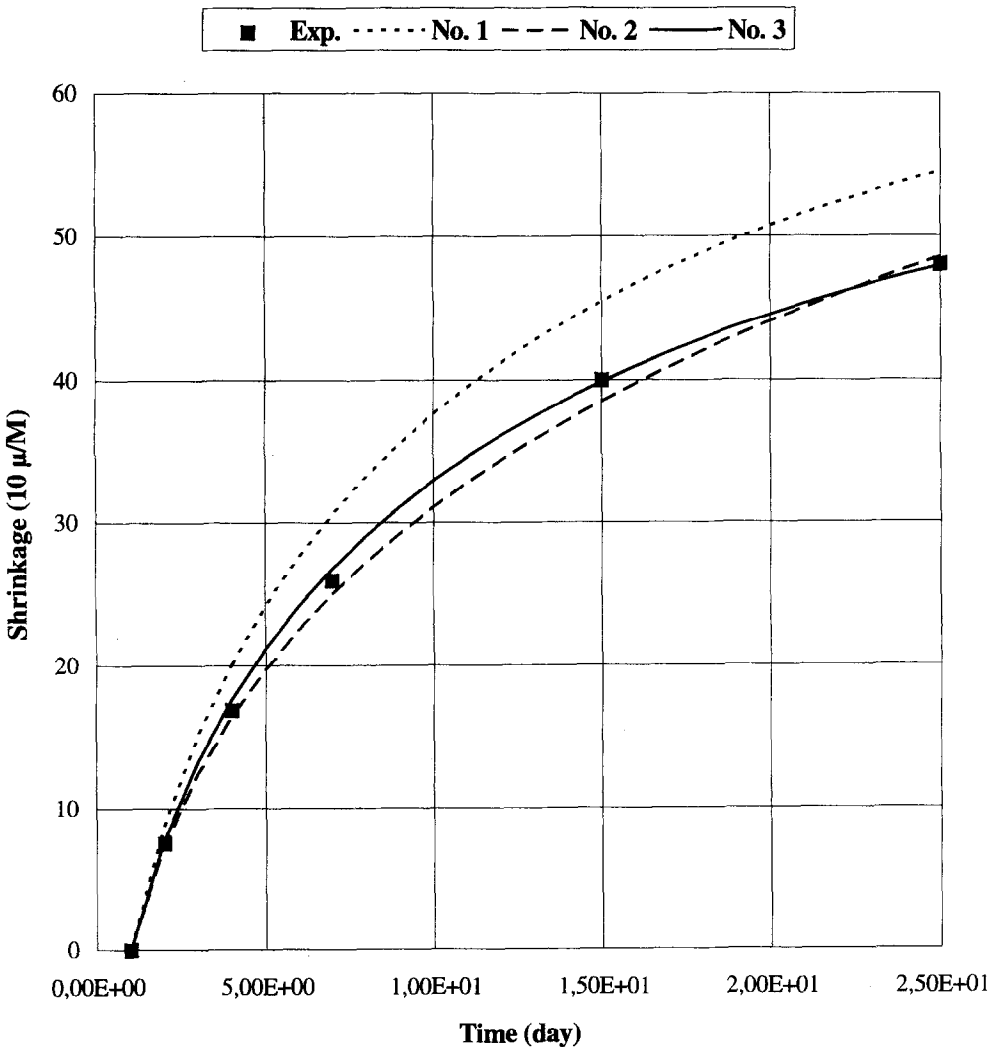


FIG. 7.
Calculated curves and measured results.

Since the intrinsic creep of the cement paste (Hua/1992/ and Hua et al./1995/) can reach, in four weeks, twice the instantaneous deformation, we take for E_{h2} and θ values of the same orders:

$$E_{h2} = 20 \text{ GPa} \quad \theta = 30 \text{ days}$$

For the *Poisson's* ratio, we take a general value:

$$\nu = 0.2$$

Three groups of data have been tried (Table 2). The results are shown by curves in Figure 7. In this figure, the calculated curves are numbered and translated to the reference point ($t = 1$ day) for comparison with the measured results from the age of one day.

7. Conclusions

- Although there is a sensitivity of the results to material parameters that we do not know precisely, we can affirm that the mechanism of capillary depression gives entirely acceptable estimations of the autogenous shrinkage because these three groups of data are not far from the reality.
- The proposed calculation is a method of homogenisation of periodic medium. It allows us to model a macroscopically ageing material with constituents having very simple behaviours. The idea of this numerical modelling can be also used for the viscoelastoplastic behaviour of the cement paste under external load during hydration because we have taken into consideration the initial deformation in each hydrate layer and this initial deformation is not reversible.

Acknowledgements

This study was financed by ENPC (Ecole Nationale des Ponts et Chaussées) and LCPC (Laboratoire Central des Ponts et Chaussées) and sustained by the Geomaterials GRECO.

8. References

1. Baroghel-Bouny V./1994/ Caractérisation des pâtes de ciment et des bétons. Méthodes, analyse, interprétations. Publ. by LCPC, Paris, 468 p., 1994.
2. Christensen R.M./1979/ "Mechanics of Composite Materials". John Wiley & Sons, New York, 1979.
3. Crassous J., Charlaix E., Gayvallet H. & Loubet J.L./1993/ Experimental study of nanometric liquid bridge with a surface force apparatus. *Langmuir*, Vol. 9, No. 8, pp. 1995-1998, 1993.
4. De Larrard F. & Le Roy R./1992/ Un modèle géométrique d'homogénéisation pour les composites bi-phasiques à inclusion granulaire de large étendue. *C. R. Acad. Sci.*, T. 314, Série II, pp. 1253-1257, 1992.
5. Hua C./1992/ Analyses et modélisations du retrait d'autodessiccation de la pâte de ciment durcissante. Thèse de doctorat de l'ENPC, Paris, 1992.

6. Hua C., Acker P. & Ehrlicher A./1995/ Analyses and modellings of the autogenous shrinkage of hardening cement paste -- I. modelling at macroscopic scale. *Cement and Concrete Research*, Vol. 25, No. 7, pp. 1457-1468, 1995.
7. Jennings H.M./1983/ The developing microstructure in portland cement. *Advances in cement technology*, Edited by Ghosh S.N., pp. 349-396, 1983.
8. Powers T.C./1960/ Properties of cement paste and concrete - Paper V-1. Physical properties of cement paste. *Proc. Fourth Int. Symp. Chemistry of Cement*, pp. 577-609, 1960.
9. Powers T.C./1965/ Mechanisms of shrinkage and reversible creep of hardened cement paste. *Proc. Int. Symp. Struct. Concr. London*, pp. 319-344, 1965.
10. Roelfstra P.E./1988/ "Numerical Concrete". Thèse de Docteur ès Sciences de l'EPFL, Lausanne, 1988.
11. Tazawa E. & Miyazawa S./1993/ Autogenous shrinkage of concrete and its importance in concrete technology. Creep and shrinkage of concrete, *Proceedings of the Fifth Internat. Symposium*, Edited by Bazant Z.P., pp. 159-168, E&FN Spon, London, 1993.
12. Wittmann F.H./1976/ The structure of hardened cement paste-a basis for a better understanding of the materials properties. *Proc. Int. Conf. Hydraulic Cement Pastes: their structure and properties*, Sheffield, pp. 96-117, 1976.